A 3D visco-elasto-plasto damage constitutive model of concrete under long-term effects

Beaudin Freinrich Dongmo[1, a *], Gianluca Mazzucco[1, b], Beatrice Pomaro[1, c], Jiangkun Zhang[1, d], Carmelo Majorana[1, e], and Valentina Salomoni[2, f]

[1]Department of Civil, Environmental and Architectural Engineering (DICEA),

University of Padova, via F. Marzolo 9, 35131, Padova, Italy

[2]Department of Management and Engineering (DTG), University of Padova,

Stradella S. Nicola 3, 36100, Vicenza, Italy

[a]beaudinfreinrich.dongmo@phd.unipd.it, [b]gianluca.mazzucco@unipd.it,
[c]beatrice.pomaro@unipd.it, [d]jiangkun.zhang@phd.unipd.it, [e]carmelo.maiorana@unipd.it,
[f]valentina.salomoni@unipd.it

Keywords: Visco-Elasto-Plasto-Damage, Long-Term Effects, Concrete, Creep

Abstract. A comprehensive 3D visco-elasto-plasto-damage constitutive model of concrete is proposed to analyze its behaviour under long-term and cyclic loadings. This model combines the visco-elasticy and plasticity theories together with damage mechanics. The work aims at providing an efficient model capable of predicting the material behaviour, taking into account time-dependent effects at the mesoscale. The visco-elastic part is modeled within the framework of the linear visco-elasticity theory. The creep function is evaluated with the aid of the B3 model by Bažant and Baweja, and implemented via the exponential algorithm. The modified Menétrey-Willam pressure-dependent yield surface, and a non-associated flow rule are used for the plastic formulation of the model. The damage part of the model considers two exponential damage parameters: one in tension, and one in compression, that account for a realistic description of the transition from tensile to compressive failure. After discussing the numerical implementation, the proposed model is calibrated, and numerical results at the mesoscale level are compared to experimental results.

Introduction

The calculation of creep deformations under long-term loading is crucial to ensure the functionality and the durability of concrete structures. Moreover, for a comprehensive description of the mechanical behaviour of concrete, nonlinear characteristics, such as stiffness degradation and reduction of strength, must be considered altogether with creep deformations. In the past and recent years, many researchers have combined various plasticity and damage models with creep models in order to reproduce accurately the phenomenological behavior of concrete. In 1998, Majorana et al. [1] consider a Maxwell chain model to combine creep with a scalar isotropic damage model. Ren et al. [2] have proposed a creep-damage-plasticity model based on strain additivity, in which an energy-based damage-plasticity model and a modified ACI model are combined together. Yu et al. [3] have studied the nonlinear creep failure of concrete by combining a Mazars' damage model [4] with the B3 creep model proposed by Bažant and Baweja. However, the coupling mechanism between these various models has not yet been fully revealed, and there is a need to use the most recent models in literature which allow for a more realistic description of concrete nonlinear behaviour.

In this paper, a comprehensive 3D visco-plasto-damage model is proposed. The plasto-damage model based on Menétrey-Willam pressure-dependent yield surface [5,6], and a non-associated flow rule is coupled with the B3 creep model of Bažant and Baweja [7]. The damage part of the model considers two exponential damage parameters, one in tension, and one in compression, that help accounting for crack closure and stiffness increase during the transition from tensile to compressive loading [8]. After calibration of the unified model, numerical simulations are performed and compared with experimental data. It is proved that the new model is capable of reproducing with satisfactory precision the nonlinear characteristics of concrete under long-term loading.

The visco-plasto-damage model

The Plasto-Damage Model. The plasto-damage model implemented in this paper considers the Menétrey-Willam plastic surface [6] modified with a scalar damage variable ω that accounts for the change in shape of the plastic surface due to damage. The plastic surface is expressed through the unified coordinates (ξ,ρ,θ) in the Haigh–Westergaard (HW) stress space as

$$f = 1.5\frac{\rho^2}{(1 - \omega^2)f_c^2} + \frac{q_h(\kappa)m}{(1-\omega)f_c}\left[\frac{\rho}{\sqrt{6}}r(\theta,e) + \frac{\xi}{\sqrt{3}}\right] - q_h(\kappa)q_s(\kappa) \leq 0, \tag{1}$$

where κ is the internal variable for plastic evolution, taken as the volumetric component of the plastic strain such that $\dot{\kappa}(\dot{\varepsilon}^p) = \mathrm{tr}(\dot{\varepsilon}^p)$. The shape of the deviatoric section is controlled by the elliptic function r(θ,e), where θ is the Lode angle, and e is the eccentricity parameter; m is the cohesion parameter, and f_c the concrete strength in compression; q_h and q_s represent the hardening and softening laws, respectively, as defined in [9].

A non-associated flow rule has been adopted, and is defined in agreement with

$$\dot{\varepsilon}_p = \dot{\lambda}\frac{\partial g_p}{\partial \sigma}(\sigma,\kappa), \tag{2}$$

where $\dot{\varepsilon}_p$ is the rate of the plastic strain, and $\dot{\lambda}$ is the plastic multiplier; κ is the internal variable defined above. The function g_p represents the plastic potential, expressed using the coordinates in the HW stress space as [8]

$$g_p = -\frac{A}{f_c}\left(\frac{\rho}{\sqrt{q(\kappa)}}\right)^2 - B\left(\frac{\rho}{\sqrt{q(\kappa)}}\right) + \frac{\xi}{\sqrt{q(\kappa)}} = 0, \tag{3}$$

where A and B are experimentally derived coefficients; f_c is the concrete strength in compression, and q(κ) is the hardening/softening law, defined as $q(\kappa) = q_h(\kappa)q_s(\kappa)$.

Damage has been considered via a total damage parameter that includes a stiffness recovery function able to catch the increase of stiffness due to closure of cracks when the mechanical loading changes from tension to compression. It is defined as a combination of the compressive and tensile damage parameters as follows

$$\omega = 1 - [1 - \omega_c(\kappa_c)][1 - s(\sigma^{tr})\omega_t(\kappa_t)], \tag{4}$$

where the scalar damage variables ω_c and ω_t are defined using exponential functions as suggested by Pijaudier-Cabot and Mazars [4]; κ_c and κ_t are internal variables used to describe the damage evolution in compression and tension, respectively, and $s(\sigma^{tr})$ is the stiffness recovery function.

The Creep Model. Herein, the creep model used to describe the long-term behaviour of concrete is the linear viscoelastic B3 model proposed by Bažant and Baweja [7]. The compliance function of the B3 creep model is expressed as

$$J(t, t') = q_1 + C_0(t, t') + C_d(t, t', t_0), \tag{5}$$

where q_1 is the instantaneous strain due to unit stress; t and t′ represent the current age, and loading age, respectively.

In Eq. 5 $C_0(t,t')$ is the basic creep term of the B3 model, expressed as [7]

$$C_0(t,t') = q_2 Q(t,t') + q_3 \ln[1 + (t-t')^{0.1}] + q_4 \ln\left(\frac{t}{t'}\right), \tag{6}$$

while $C_d(t, t', t_0)$ is the drying creep term of the B3 model expressed as [7]

$$C_d(t,t',t_0) = q_5 \left[e^{-8H(t)} - e^{-8H(t_0')}\right]^{0.5}, \tag{7}$$

where t_0 is the time at which drying starts, and $t_0' = \max(t', t_0)$; $H(t)$ and $H(t_0')$ are spatial averages of pore relative humidity [7].

The parameters q_1 to q_5 can be approximated via empirical formulas [7]. The creep model is implemented via the exponential algorithm [10].

Numerical results

In the scope of this paper, 3D mescoscale models of ordinary concrete made by calcareous aggregates have been reconstructed using 3D computed tomography. In the mesoscale models, the aggregates are modelled as elastic; the cement paste has been modelled using the above mentioned visco-plasto-damage model. A sketch of the adopted solid model is represented in Fig. 1 (left).

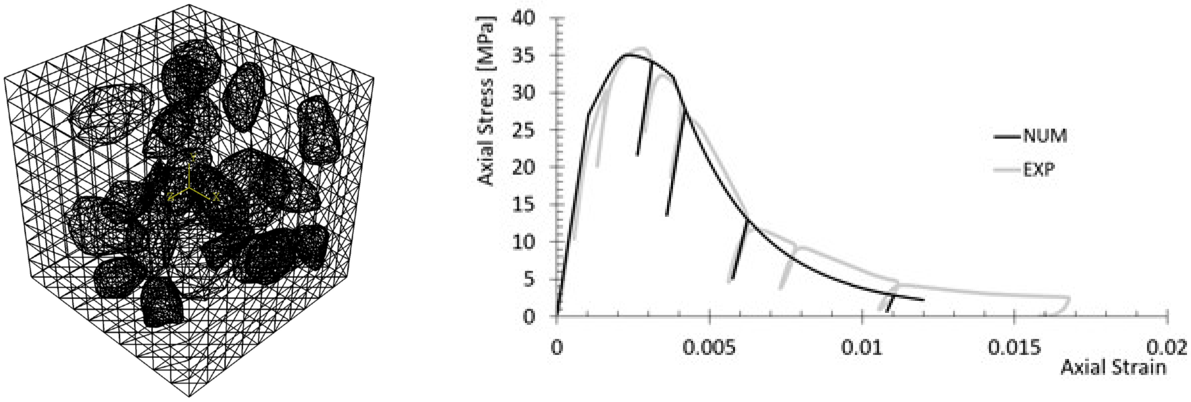

Figure 1: 3D sample reconstruction (left), and comparison between numerical and experimental results of the uniaxial compression test (right).

The calibration of the model has been conducted over experimental results obtained from a uniaxial compression test with loading and unloading cycles, on a cubic sample of same geometry and grading curve of the adopted model. Subsequently, similar experiments considering short- and long-term loadings have been considered for validation of the present model. In particular, the two parameters A and B of the plastic potential are determined by means of the axial strain in uniaxial compression at maximum stress and the axial strain in triaxial compression at maximum stress, as illustrated in [9]. The elasto-plasto-damaged parameters for cement matrix constituent are reported in Table 1.

Table 1: Elasto-pasto-damage parameters after calibration.

ELASTO-PLASTICITY			DAMAGE		
E	Young modulus at 28 days [MPa]	33,000	k_{c0}	1D initial inelastic strain for compression damage	0.015
ν	Poisson's ratio	0.2	A_c	Damage parameter in compression	1
f_c	Compressive strength at 28 days [MPa]	34.6	B_c	Damage parameter in compression	100
f_t	Traction strength at 28 days [MPa]	3.5	$\omega_{c\ max}$	Maximum damage in compression	0.95
e	Eccentricity	0.55	k_{t0}	1D initial inelastic strain for tension damage	0.0015
t	Slope for the softening function q_s	0.003	A_t	Damage parameter in tension	1
k_{1D}	Plastic strain in the compressive pick	0.1	B_t	Damage parameter in tension	1
q_{h0}	Initial hardening function q_h	0.4	$\omega_{t,max}$	Maximum damage in tension	0.95
A	Plastic potential parameter	-2.22	s_0	Maximum recovery value	0.2
B	Plastic potential parameter	-3.46	G_f	Fracture energy [10^3J/m^2]	0.025
			w_c	Crack bands width [mm]	1

Fig. 1 (right) reports the comparison between numerical and experimental results for the short-term loading with loading and unloading cycles. The model proves to reproduce satisfactorily the post-peak behaviour and stiffness degradation during the softening regime.

The comparison between numerical and experimental results for the long-term loading is shown in Fig. 2. Also in this case the numerical results are in good agreement with the experimental ones.

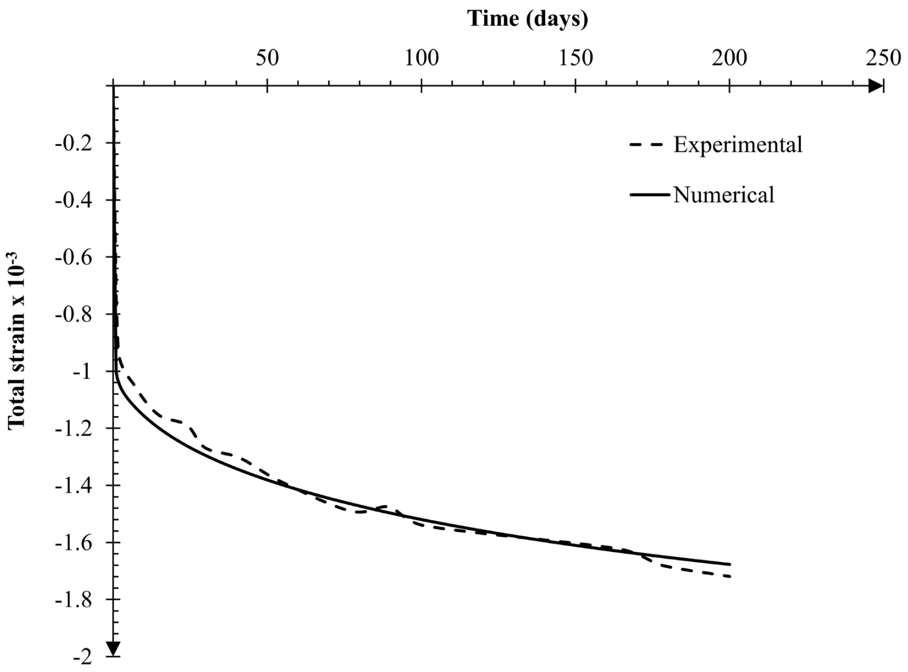

Figure 2: Comparison between numerical and experimental results of the creep test.

Fig. 3 shows the stress distribution in the direction of the load, across the sample. Overall, stress localizations in the regions of the cement paste surrounding the aggregates are envisaged. This is coherent with the expected triggering of damage at the interface zone between aggregates and cement paste, and subsequent failure following these preferential paths.

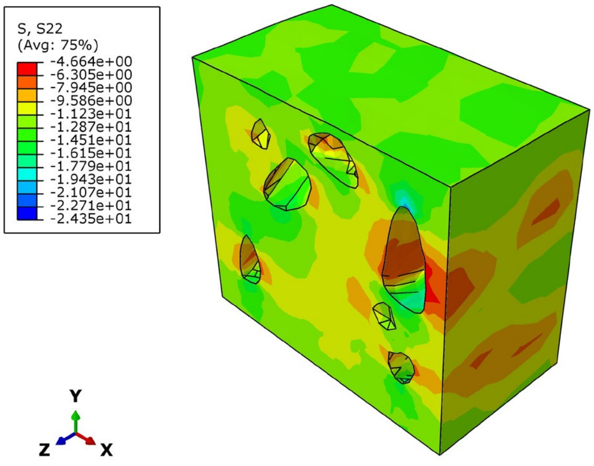

Figure 3: Stress contour map (in MPa) in the cement paste.

Summary

The comprehensive 3D visco-plasto-damage model presented herein combines a pressure-dependent plastic model extended to include damage with a linear visco-elastic creep model for the study of the coupling mechanism between creep and damage. Specifically, the plasto-damage model includes a pressure-dependent yield surface and a stiffness recovery function for a more realistic description of the transition from tensile to compressive failure. The creep model considers two contributions: a basic creep, and drying creep. After calibration and validation of the model, a numerical simulation has been conducted on a cubic concrete sample at the mesoscale, undergoing creep. The comparison between numerical and experimental results confirms that the proposed unified model is capable of characterizing accurately the nonlinear material behaviour of concrete under short and sustained loading.

References

[1] C. E. Majorana, V. Salomoni, B. A. Schrefler, Hygrothermal and mechanical model of concrete at high temperature, Materials and structures 31(1998) 378-386. https://doi.org/10.1007/BF02480710

[2] X. Ren, Q. Wang, R. Ballarini, X. Gao, Coupled creep-damage-plasticity model for concrete under long-term loading, Journal of Engineering Mechanics 146 (2020) 04020027. https://doi.org/10.1061/(ASCE)EM.1943-7889.0001748

[3] P. Yu, R. Li, D. Bie, X. Yao, X. Liu, Y. Duan, A coupled creep and damage model of concrete considering rate effect, Journal of Building Engineering 45 (2022) 103621. https://doi.org/10.1016/j.jobe.2021.103621

[4] G. Pijaudier-Cabot, J. Mazars, Handbook of materials behavior models, three-volume set, Elsevier, 2001.

[5] G. Mazzucco, B. Pomaro, G. Xotta, C. E. Maiorana, V. A. Salomoni, Tomography reconstruction of concrete materials for mesoscale modelling, Engineering Computations 37 (2020) 2275–2291. https://doi.org/10.1108/EC-10-2019-0448

[6] P. Menétrey, K.J. Willam, Triaxial failure criterion for concrete and its generalization, Structural Journal 92 (1995) 311–318. https://doi.org/10.14359/1132

[7] Z. P. Bažant, S. Baweja, Creep and shrinkage prediction model for analysis and design of concrete structures: Model b3, ACI Special Publications 194 (2000) 1–84.

[8] P. Grassl, D. Xenos, U. Nyström, R. Rempling, K. Gylltoft, Cdpm2: A damage-plasticity approach to modelling the failure of concrete, International Journal of Solids and Structures 50 (2013) 3805–3816. https://doi.org/10.1016/j.ijsolstr.2013.07.008

[9] P. Grassl, K. Lundgren, K. Gylltoft, Concrete in compression: a plasticity theory with a novel hardening law, International Journal of Solids and Structures 39 (2002) 5205–5223. https://doi.org/10.1016/S0020-7683(02)00408-0

[10] Q. Yu, Z. P. Bažant, R. Wendner, Improved algorithm for efficient and realistic creep analysis of large creep-sensitive concrete structures, ACI Structural Journal 109 (2012) 665. https://doi.org/10.14359/51684044